IRSTI 29.19.27, 53.47.23 https://doi.org/10.26577/phst20251227

Study of thermoelectric properties of tungsten silicides

A.T. Mamadalimov[1], M.Sh. Isaev[2, 3*], S.R. Qodirov[4], N.K. Khakimova[1] and I.A. Mengliev[5]

[1]Institute of Semiconductor Physics and Microelectronics, Tashkent, Uzbekistan
[2]National University of Uzbekistan named after Mirzo Ulugbek, Tashkent, Uzbekistan
[3]Cyber University of Uzbekistan, Tashkent, Uzbekistan
[4]Urgench State University, Urgench, Uzbekistan
[5]Tashkent State University of Transport, Tashkent, Uzbekistan
*e-mail: isayevmahmud02@gmail.com

(Received September 22, 2025; received in revised form December 11, 2025; accepted December 15, 2025)

This work presents a comprehensive investigation of the temperature-dependent electrical and thermal transport properties of tungsten silicides, including mono-, di-, and higher-order phases. A comparative analysis of experimental data is performed with particular emphasis on electronic structure, charge-carrier characteristics, and phase-dependent transport behavior. The results indicate that di- and higher-order tungsten silicides exhibit semiconductor-like properties, with electrical resistivities in the range of 50–85 μΩ·cm at 300 K. Nuclear magnetic resonance spectroscopy was employed to examine the local electronic environment of tungsten atoms and their interaction with surrounding silicon nuclei, revealing structural imperfections such as defects, grain boundaries, and secondary-phase inclusions that influence charge transport. The temperature dependences of electrical conductivity, thermal conductivity, Seebeck coefficient, and thermoelectric quality factor were systematically studied over the temperature range of 300–800 K. The analysis demonstrates that higher-order tungsten silicides exhibit the most favorable thermoelectric characteristics among the investigated phases, highlighting their potential for use in high-temperature thermoelectric energy conversion and sensing applications, as well as their promise for further optimization through controlled doping strategies.

Keywords: tungsten silicide, diffusion, phase analytics, electrical conductivity, thermal conductivity, thermoEMF.
PACS number(s): 72.20.Pa, 72.15.Jf, 72.80.Ga.

1. Introduction

Tungsten silicides synthesized via diffusion doping of monocrystalline silicon are promising materials for applications in micro- and nanoelectronics as well as solar engineering, owing to their high thermal stability, excellent electrical conductivity, and strong resistance to oxidation [1–4]. Transition metal silicides, particularly those based on tungsten, constitute an important class of intermetallic compounds that are widely employed in silicon-based technologies due to their compatibility with standard fabrication processes, chemical stability, and favorable electronic properties.

Beyond their established use in electrical contacts and Schottky barrier structures, tungsten silicides have attracted increasing interest as potential thermoelectric materials. The performance of thermoelectric materials is commonly evaluated using the dimensionless figure of merit Q=ZT, which depends on the Seebeck coefficient α, electrical conductivity σ and thermal conductivity æ, and is expressed as:

$$Q = \frac{\alpha^2 \sigma T}{æ}. \quad (1)$$

A deep understanding of the thermoelectric behavior of tungsten silicides is essential for the development of miniaturized temperature sensors and solid-state energy conversion devices [5].

Among the wide range of thermoelectric materials investigated, transition metal silicides–particularly tungsten silicide phases such as WSi_2 and W_5Si_3 have garnered special attention. These materials offer several advantages, including high-temperature sta-

bility, resistance to oxidation, relatively low cost, and environmental compatibility compared with conventional thermoelectric compounds based on tellurium or lead [6–8].

Despite these advantages, the thermoelectric properties of tungsten silicides remain insufficiently explored. Improving their thermoelectric efficiency requires a detailed analysis of their electronic structure and thermal transport behavior, as well as an understanding of the influence of phase composition, microstructure, and doping. In this paper, we investigate the thermoelectric properties of various tungsten silicide phases to evaluate their potential for application in high-temperature thermoelectric energy converters [9–12].

Tungsten silicides are promising materials for high-temperature thermoelectric applications due to their unique combination of structural stability, electronic properties, and thermal characteristics. Despite numerous studies on individual properties of tungsten silicides, there remains a lack of comprehensive understanding of how their crystal structure, defect states, and electronic environment collectively influence their thermoelectric performance [13-15].

The aim of this study is a comprehensive investigation of the formation, structure, defect states, and electronic properties of mono-, di-, and higher-order tungsten silicides, as well as their thermoelectric characteristics, with the goal of identifying the phases most promising for high-temperature thermoelectric converters.

The novelty of this work lies in its integrated approach: we simultaneously investigate the formation, crystalline structure, microstructural defects, electronic conductivity, and thermoelectric properties of various tungsten silicides. By correlating structural features and electronic behavior with thermoelectric performance, this study provides a detailed understanding of the material's behavior and identifies the specific tungsten silicide phases most suitable for high-temperature thermoelectric devices.

This research therefore bridges the gap between fundamental materials characterization and applied thermoelectric performance, offering new insights into the design of advanced materials for high-temperature energy conversion.

2. Experimental

Tungsten silicides of different stoichiometries (WSi, WSi_2, and W_5Si_3) were synthesized by solid-state diffusion between high-purity tungsten and single-crystal silicon substrates. The samples were prepared in a horizontal diffusion furnace (SUOL-4 type). The diffusion process was carried out at temperatures between 1000 and 1200 °C for 40–45 hours, conditions chosen to ensure the formation of monosilicide, disilicide, and higher silicide phases, as observed in previous studies of tungsten–silicon phase interactions. After diffusion annealing, the samples were cooled to room temperature inside the furnace to minimize thermal stresses.

The phase composition and crystal structure of the synthesized silicides were investigated using X-ray diffraction (XRD) using Cu Kα radiation. Diffraction patterns were collected in the 2θ range of 20–80°. Lattice parameters for each phase were refined using the Rietveld method. The obtained structural characteristics were found to correlate directly with the differences in thermal and electronic transport properties discussed later, particularly the increased structural complexity of the W_5Si_3 phase, which contributes to enhanced phonon scattering and, consequently, reduced thermal conductivity.

To analyze the local chemical environment of silicon atoms within each phase, ^{29}Si Nuclear Magnetic Resonance (NMR) spectroscopy was performed. The spectra were recorded at room temperature using a standard solid-state NMR setup with magic-angle spinning (MAS). Distinct chemical shifts and line broadening were used to distinguish between silicon sites in WSi, WSi_2, and W_5Si_3. Broadened lines in the higher silicide phase indicated the presence of multiple non-equivalent silicon sites and structural defects, which later manifested in enhanced phonon scattering and reduced thermal conductivity.

Electrical conductivity (σ) was measured in the temperature range 300–800 K using the standard four-probe technique. Rectangular specimens were prepared from the reacted silicide layers, and platinum leads were attached using high-temperature silver paste. Temperature stability during measurements was maintained within ±1 K. The resulting temperature dependence of σ confirmed metallic behavior for WSi and semiconducting behavior for WSi_2 and W_5Si_3, in agreement with their respective electronic structures.

Thermal conductivity (κ) was determined using the laser flash analysis (LFA) method. The thermal diffusivity (æ) was measured directly, while thermal conductivity was calculated according to

$$k = æ \cdot \rho \cdot C_p \quad (2)$$

where ρ is the density (determined by Archimedes' method) and C_p is the heat capacity (measured using differential scanning calorimetry, DSC).

This technique enabled accurate measurement of the temperature dependence of κ for all phases, revealing the lowest thermal conductivity for W_5Si_3 due to its complex tetragonal structure and higher defect concentration.

The Seebeck coefficient (α) was measured simultaneously with electrical conductivity using a differential DC method. A temperature gradient of approximately 10–15 K was applied across the sample, and the resulting thermoelectric voltage was recorded. Measurements were repeated during heating from 300 to 800 K.

In solid-state NMR spectroscopy, chemical shift (δ) is a sensitive indicator of the electron density around the nucleus. A strongly negative δ value typically corresponds to high levels of shielding, characteristic of metallic systems. A broad spectral line indicates electron inhomogeneity, as well as the influence of shielding anisotropy. The structures of W_5Si_2 and W_5Si_3 belong to different types of intermetallic compounds, resulting in different environments for the silicon atoms. The study was conducted using a Varian Mercury VX-400 NMR system.

This approach captured the expected monotonic increase of α with temperature and showed the highest Seebeck coefficient in W_5Si_3, consistent with its semiconducting nature and enhanced density of states near the Fermi level.

3. Results and discussion

The electrical conductivity, thermal conductivity and coefficient of thermo-EMF were measured in the temperature range of 300-800 K using standard techniques.

Fig. 1 shows the temperature dependence of the electrical conductivity of mono-, di- and higher silicides of tungsten. A noticeable decrease in electrical conductivity is observed for all tungsten silicide phases in Fig. 1. This trend is consistent with the expected increase in phonon scattering at elevated temperatures, which reduces charge-carrier mobility and thus lowers the overall conductivity.

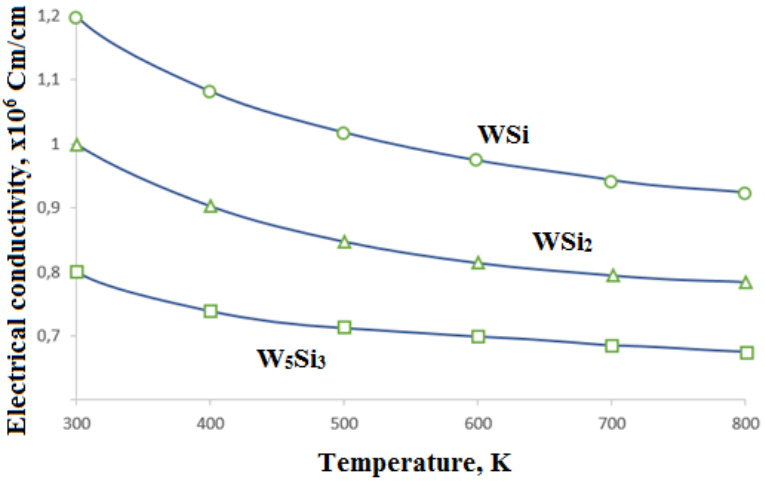

Figure 1 – Temperature dependences of electrical conductivity of various phases of tungsten silicides.

Tungsten monosilicide has the highest electrical conductivity, which is due to its metallic nature and dense crystal lattice [16]. The tungsten dilicide behaves as a semiconductor and takes an intermediate value between the electrical conductivity of the mono- and higher tungsten silicide. The highest tungsten silicide has a minimum electrical conductivity, characteristic of a more silicon phase with semiconductor properties [17,18].

Fig. 2 shows the temperature dependence of thermal conductivity of various phases of tungsten silicides. In all three phases, a decrease in thermal conductivity with an increase in temperature is observed due to increased phonon-phonon scattering [19].

Monosilicide has the highest thermal conductivity (æ = 80 W/m • K at T = 300 K) – a dense crystalline structure and high contribution of the electronic component. The smallest thermal conductivity (æ = 24 W/m • K at T = 300 K) is also observed in higher tungsten silicide.

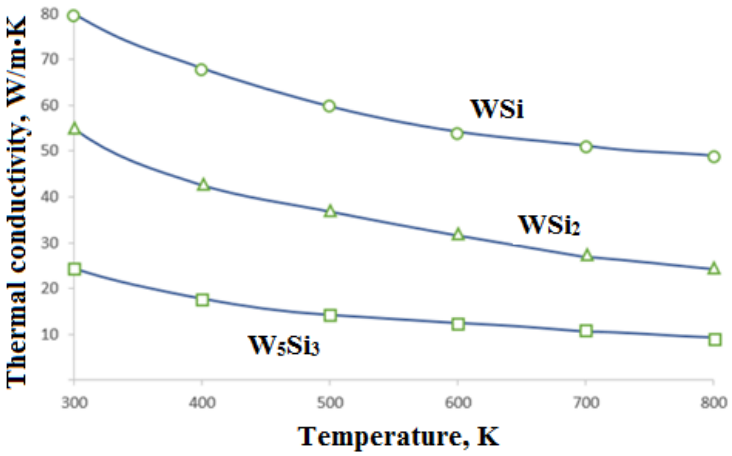

Figure 2 – Temperature dependences of thermal conductivity various phases of tungsten silicides.

The disilicide of the tungsten is æ = f (t) occupies an intermediate value (æ = 56 W/m • K at T = 300 K). Less thermal conductivity of the di- and higher tungsten silicide is due to their complex structure and an increase in scattering at the phonons, on grains boundaries and defects of the crystal lattice [20,21].

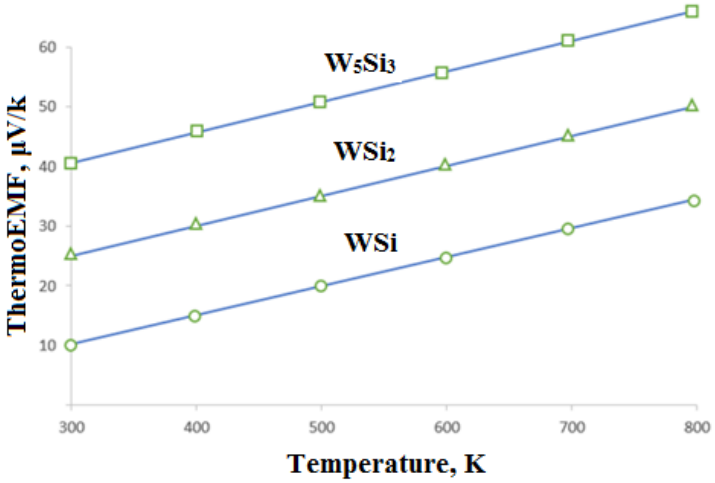

Figure 3 – Temperature dependences of the coefficient of thermoEMF of various phases of tungsten silicides.

Fig. 3 shows the temperature dependence of the coefficient of thermoEMF of various phases of tungsten silicides. With an increase in temperature, the thermoEMF coefficient increases, which is typical for semiconductors and metals with a high density of states at the level of Fermi. The highest silicide of tungsten α = 40 to 60 μV/k, which is associated with its more pronounced semicon-

ductor properties [22]. The tungsten dilicide has α = 25 μV/k (at T = 300 K) to 48 μV/k (at T = 800 K). Monosilicide demonstrates the smallest coefficient: α = 25 μV/k (at T = 300 K) up to 30 μV/k (at T = 800 K), which is characteristic of metal phases [23].

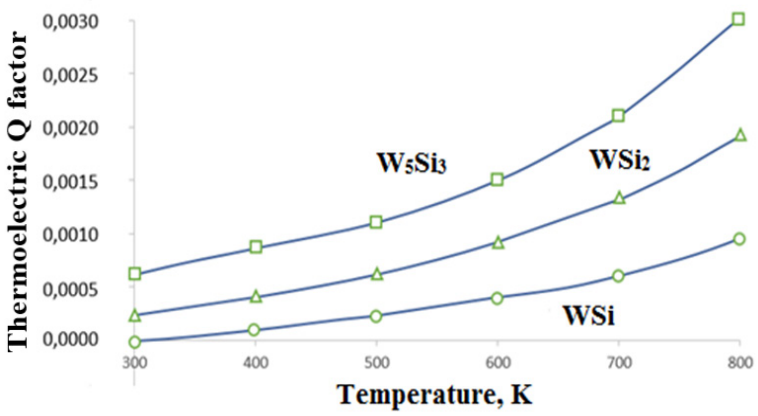

Figure 4 – Temperature dependencies of thermoelectric Q factor for various phases of tungsten silicides.

Fig. 4 shows the temperature dependence of thermoelectric Q factor Q = ZT. This parameter depends on the coefficient of thermoEMF, electrical conductivity and thermal conductivity. The maximum value of thermoelectric quality is observed in the highest silicide of the tungsten [24,25]. In this phase of tungsten silicides, despite the low electrical conductivity (Fig. 1), the high Seebeck coefficient (Fig. 3) and low thermal conductivity (Fig. 2) provides improved thermoelectric properties. The highest values of the Seebeck coefficient are observed in the highest silicide of the tungsten due to the fact that it increases the energy gap and density of states near the level of farm. This phase is a promising material for thermoelectric converters. The monosilicide of the tungsten shows the low values of Q-due to the low coefficient of thermoEMF and high thermal conductivity.

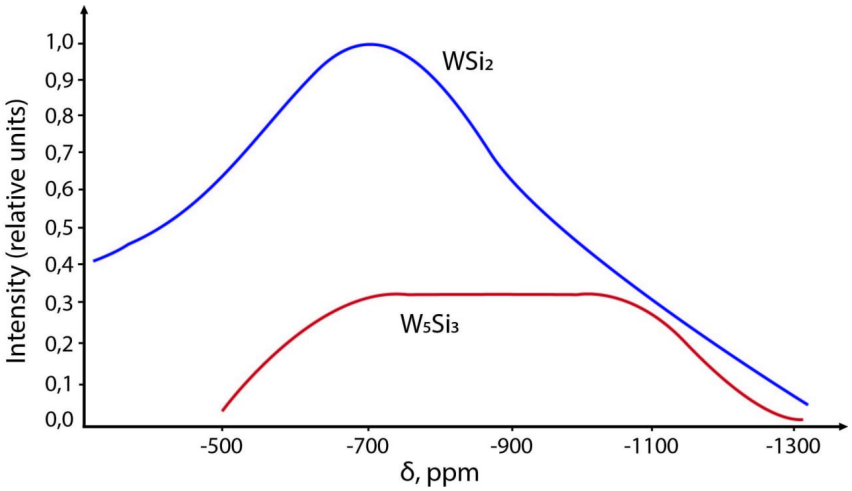

Figure 5 – NMR spectra of WSi_2 and W_5Si_2.

Fig.5 shows the relative signal intensity (Y-axis) as a function of the chemical shift δ (ppm, X-axis) for two tungsten silicides. The solid-state ^{29}Si NMR spectra clearly distinguish the silicon environments in the phases WSi_2 and W_5Si_3, allowing their structural and electronic features to be compared. The spectrum of WSi_2 exhibits a pronounced and relatively symmetric maximum in the region of –700 to –900 ppm, with high relative intensity. This indicates a narrow distribution of local electronic environments around silicon, consistent with a well-ordered crystal structure and the predominance of a single crystallographic Si site. The negative chemical shift is governed by a substantial Knight shift contribution, resulting from the high density of conduction electrons associated with tungsten.

In contrast, the spectrum of W_5Si_3 appears as a broad, asymmetric band extending toward –1100 to –1200 ppm, with substantially lower intensity. Such line broadening reflects the presence of multiple non-equivalent Si sites and a pronounced heterogeneity of local electronic states. The more negative chemical shift values indicate an enhanced metallic character of this phase, leading to a stronger Knight shift contribution. The overall broad signal width confirms a wide distribution of electron density on silicon atoms, which is characteristic of silicides with higher degrees of metal–metal interaction.

Thus, the comparative analysis of the spectra shows that WSi_2 possesses a more ordered structure with a narrower shielding distribution, while W_5Si_3 exhibits significant electronic and structural heterogeneity, resulting in substantial line broadening and a shift of the resonance toward more negative values.

Solid-state ^{29}Si NMR spectroscopy is a powerful tool for probing the local electronic environments in transition-metal silicides, where the chemical shift is strongly influenced by conduction-electron density, metal–metal bonding, and the number of crystallographically distinct Si sites. Previous systematic studies [26] have shown that ^{29}Si isotropic shifts in such compounds may span a remarkably wide range, from moderately negative values (−200 to −600 ppm) in weakly metallic silicides to highly negative shifts reaching −1000 ppm or more in phases with pronounced metallic behavior. This broad variation is primarily attributed to the Knight shift, which reflects the Fermi-contact interaction between the conduction electrons of the transition metal and the silicon nuclei. Consequently, heavy transition-metal silicides containing W, Mo, Re, or Ru typically exhibit the most negative shifts, along with significant line broadening.

The present NMR results align well with these established trends. The ^{29}Si spectrum of WSi_2 shows a relatively sharp and symmetric resonance centered between −700 and −900 ppm. Such a line shape is characteristic of phases with a well-ordered crystal structure and a single dominant Si site, resulting in a narrow distribution of local electronic environments. Comparable chemical-shift magnitudes have been reported for structurally ordered disilicides such as $MoSi_2$ and $RuSi_2$, which also exhibit moderate Knight-shift contributions while retaining a relatively uniform electronic environment.

In contrast, the spectrum of W_5Si_3 displays a broad, asymmetric resonance extending to much more negative values (approximately −1100 to −1200 ppm). This behavior is fully consistent with earlier observations for higher-order transition-metal silicides [27,28], where multiple non-equivalent Si sites, enhanced metallicity, and strong metal–metal interactions lead to a large Knight shift as well as substantial broadening of the spectral line. Such a broadened resonance typically reflects a wide distribution of conduction-electron density at the Si sites, arising from both intrinsic structural complexity and electronic heterogeneity. Furthermore, studies employing temperature-dependent ^{29}Si NMR [29] have demonstrated that highly metallic silicides often exhibit pronounced shift anisotropy and strong sensitivity to structural defects, grain boundaries, and site disorder–features also consistent with the line broadening observed in W_5Si_3.

The obtained results are consistent with the general understanding of charge and heat transport mechanisms in transition-metal silicides and agree well with previously published data [30-32]. The measured temperature dependence of electrical conductivity shows a monotonic decrease of σ with increasing temperature for all phases studied. This behavior is typical for materials in which phonon scattering dominates at elevated temperatures. Similar σ(T) trends were previously reported for $MoSi_2$, $TaSi_2$, and WSi_2 by [30], confirming the universal nature of phonon-limited transport in silicides with rigid crystal lattices.

The metallic behavior of monosilicide WSi can be attributed to the presence of dense d-bands near the Fermi level, which ensure high carrier mobility. According to earlier studies on monosilicides of transition metals (WSi, MoSi, TiSi), these phases typically exhibit very low Seebeck coefficients due to the predominant electronic contribution to conductivity [30,31]. Our results fully support these findings: the

Seebeck coefficient of WSi remains within 25–30 μV/K over the 300–800 K temperature range.

Tungsten disilicide WSi_2 shows behavior characteristic of a narrow-band semiconductor. The performed NMR analysis reveals a highly symmetric silicon environment and broader spectral lines compared to WSi, in agreement with literature data on partially ordered silicon sublattices in disilicides [31]. As previously noted by [31], semiconductor-like disilicides display an increase in the Seebeck coefficient with temperature. This trend is also observed here: α increases by nearly a factor of two between 300 and 800 K.

The most noteworthy behavior is observed in the higher tungsten silicide W_5Si_3. According to the results, this phase exhibits the lowest thermal conductivity and the highest Seebeck coefficient among the materials studied. A similar effect was reported by [32] for Nb- and Ta-doped W_5Si_3, where reduced thermal conductivity was attributed to the complexity of the crystal structure and enhanced phonon scattering at structural defects. Our NMR data, showing multiple nonequivalent silicon sites and broadened spectral lines, also indicate defect-rich local environments, which likely contribute to the observed suppression of lattice thermal conductivity.

A promising direction for further improvement of the thermoelectric performance of WSi_2 and W_5Si_3 is doping with transition metals such as Nb, Ta, or Re. Previous studies [32] have shown that doping enhances phonon scattering and can significantly increase ZT. The defect-related features revealed by our NMR measurements also suggest that controlled manipulation of structural disorder and point defects could serve as an effective tool for optimizing the thermoelectric properties of tungsten silicides.

4. Conclusion

In this study, the formation and properties of tungsten silicides were comprehensively investigated. Using X-ray diffraction, scanning electron microscopy, and nuclear magnetic resonance techniques, the formation of mono-, di-, and higher-order tungsten silicides was confirmed during diffusion annealing at temperatures ranging from 850 to 1000 °C. The study demonstrated the formation of intermetallic compounds, specifically identifying mono-, di-, and higher tungsten silicides, with their crystalline structures characterized and lattice parameters determined.

The electronic properties of these silicides were also examined. It was found that the di- and higher-order tungsten silicides exhibit semiconductor-type conductivity, with specific resistances measured at 50–85 μΩ·cm at 300 K. Nuclear magnetic resonance (NMR) spectra provided insights into the influence of the tungsten electronic environment on the silicon nucleus, revealing the presence of defects, grain boundaries, and inclusions. These structural imperfections were reflected in the spectral lines, contributing to the understanding of the material's microstructure.

Thermoelectric performance was evaluated through temperature-dependent measurements of electrical conductivity, thermal conductivity, the Seebeck coefficient, and thermodynamic volume in the range of 300–800 K. Among the tungsten silicides studied, the highest-order silicide exhibited the most favorable thermoelectric properties, indicating its potential as a promising candidate for high-temperature thermoelectric energy conversion applications. The WSi_2 phase exhibits a relatively narrow and symmetric resonance in the region of –700 to –900 ppm, indicating a more ordered silicon environment with a single dominant crystallographic site. In contrast, the spectrum of W_5Si_3 is significantly broader and shifted toward more negative chemical shift values (down to –1200 ppm), reflecting a higher degree of structural and electronic heterogeneity and multiple non-equivalent Si positions.

Overall, the results provide a detailed understanding of the structural, electronic, and thermoelectric characteristics of tungsten silicides, highlighting their suitability for advanced thermoelectric devices operating at elevated temperatures.

References

1. Utamuradova Sh.B., Rakhmanov D.A., Tuan P.L., Doroshkevich A.S., Isayev R.Sh., Abiyev A.S. Studying the influence of proton irradiation on the distribution profile of Pt and Cr in surface layers n-Si⟨Pt⟩, n-Si⟨Cr⟩ using ellipsometric spectroscopy // Advanced Physical Research. – 2024. – Vol. 6(2). – Pp. 83–89. https://doi.org/10.62476/apr62.83

2. Isaev M.Sh., Bozarov I.T., Tursunov A.I. Investigation of thermally stimulated conductivity of cobalt silicide // E3S Web of Conferences. – 2023. – Vol. 402. – Art. 14019. https://doi.org/10.1051/e3sconf/202340214019

3. Tursunov M.O., Iliev Kh.M., Ismaylov B.K. High-temperature analysis of silicon properties with manganese–oxygen binary complexes // Physical Sciences and Technology. – 2024. – Vol. 11(1–2). – Pp. 4–12. https://doi.org/10.26577/phst2024v11i1a1

4. Utamuradova Sh.B., Daliev Sh.Kh., Rakhmanov D.A., Samadov S.F., Doroshkevich A.S. Investigation of radiation defect formation of irradiated n-Si⟨Pt⟩ // Advanced Physical Research. – 2023. – Vol. 5(3). – Pp. 183–191.

5. Daliev K.S., Khusanov Z.M. Properties of single crystal silicon doped with vanadium // East European Journal of Physics. – 2024. – No. 1. – Pp. 366–369. https://doi.org/10.26565/2312-4334-2024-1-35

6. Daliev K.S., Utamuradova Sh.B., Khamdamov J.J., Bekmuratov M.B., Yusupov O.N., Norkulov Sh.B., Matchonov Kh.J. Defect formation in MIS structures based on silicon with an impurity of ytterbium // East European Journal of Physics. – 2024. – No. 4. – Pp. 301–304. https://doi.org/10.26565/2312-4334-2024-4-33

7. Kenzhaev Z.T., Iliev Kh.M., Ismailov K.A., Mavlonov G.Kh., Koveshnikov S.V., Ismaylov B.K., Isamov S.B. Physical mechanisms of gettering properties of nickel clusters in silicon solar cells // Physical Sciences and Technology. – 2024. – Vol. 11(1–2). – Pp. 13–22. https://doi.org/10.26577/phst2024v11i1a2

8. Utamuradova Sh.B., Rakhmanov D.A., Abiyev A.S. Influence of gamma rays on electrophysical properties of silicon doped with palladium atoms // Physics AUC. – 2024. – Vol. 34. – Pp. 198–203.

9. Azamatov Z.T., Yuldoshev M.A., Bazarbayev N.N., Bakhromov A.B. // Physics AUC. – 2023. – Vol. 33. – P. 139–145.

10. Utamuradova Sh.B., Rakhmanov D.A., Doroshkevich A.S., Genov I.G., Tuan P.L., Kirillov A. Processes of defect formation in silicon diffusionally doped with platinum and irradiated with protons // Eurasian Physical Technical Journal. – 2023. – Vol. 20(3). – Pp. 35–42. https://doi.org/10.31489/2023No3/35-42

11. Ayupov K.S., Zikrillaev H.F., Saitov E.B., Abdullaeva N.U., Umarkhojayeva Z.N., Yakhyayev M.M. Auto-oscillations of current in injection structures p^+–p(Si) based on heavily compensated silicon // Physical Sciences and Technology. – 2024. – Vol. 11(3–4). – Pp. 49–57. https://doi.org/10.26577/phst2024v11i2b06

12. Utamuradova Sh.B., Rakhmanov D.A., Abiyev A.S. Influence of different types of radiation on the crystal structure of silicon monocrystals n-Si // East European Journal of Physics. – 2024. – No. 2. – Pp. 380–383. https://doi.org/10.26565/2312-4334-2024-2-47

13. Abdullayev J.Sh., Sapaev I.B. Modeling and calibration of electrical features of p–n junctions based on Si and GaAs // Physical Sciences and Technology. – 2024. – Vol. 11(3–4). – Pp. 39–48. https://doi.org/10.26577/phst2024v11i2b05

14. Utamuradova Sh.B., Daliev Sh.Kh., Rakhmanov D.A., Khamidjanov I.Kh., Doroshkevich A.S., Mezentseva Zh.V., Tatarinova A. Influence of gamma rays on electrophysical properties of silicon doped with palladium atoms // Advanced Physical Research. – 2025. – Vol. 7(3). – Pp. 166–173. https://doi.org/10.62476/apr.73166

15. Ismaylov B.K., Zikrillayev N.F., Ismailov K.A., Kenzhaev Z.T. Clusters of impurity nickel atoms and their migration in the crystal lattice of silicon // Physical Sciences and Technology. – 2023. – Vol. 10(1–2). – Pp. 13–18. https://doi.org/10.26577/phst.2023.v10.i1.02a

16. Utamuradova Sh.B., Daliev Kh.S., Daliev Sh.Kh., Muzafarova S.A., Fayzullaev K.M., Muzafarova G.A. // E3S Web of Conferences. – 2024. – Vol. 583. – Art. 04006. https://doi.org/10.1051/e3sconf/202458304006

17. Nematov D., Kholmurodov Kh., Stanchik A., Fayzullaev K., Gnatovskaya V., Kudzoev T. On the optical properties of the $Cu_2ZnSn[S_1–xSe_x]_4$ system in the IR range // Trends in Sciences. – 2023. – Vol. 20(2). – Art. 4058. https://doi.org/10.48048/tis.2023.4058

18. Utamuradova Sh.B., Daliyev Sh.Kh., Khamdamov J.J., Matchonov Kh.J., Utemuratova Kh.Y. Research of the impact of silicon doping with holmium on its structure and properties using Raman scattering spectroscopy methods // East European Journal of Physics. – 2024. – No. 2. – Art. 274. https://doi.org/10.26565/2312-4334-2024-2-28

19. Mamadalimov A.T., Isaev M.Sh., Atamirzaev T.U., Ernazarov S.N., Karimov M.K. CVC structure of PtSi–Si⟨Pt⟩–M in a wide range of temperatures // East European Journal of Physics. – 2024. – No. 2. – Pp. 358–361. https://doi.org/10.26565/2312-4334-2024-2-43

20. Utamuradova Sh.B., Rakhmanov D.A., Tuan P.L., Doroshkevich A.S., Kinev V.A., Tatarinova A., Isayev R.Sh., Abiyev A.S. Influence of alpha particles on technological impurities in silicon doped with platinum // New Materials, Compounds and Applications. – 2025. – Vol. 9(1). – Pp. 50–57. https://doi.org/10.62476/nmca.9150

21. Dynys F.W., Sayir A., Mackey J., Sehirlioglu A. Thermoelectric properties of WSi_2–Si_xGe_{1-x} composites // Journal of Alloys and Compounds. – 2014. – Vol. 604. – Pp. 196–203. https://doi.org/10.1016/j.jallcom.2014.04.171

22. Rogacheva E. et al. Thermoelectric performance of silicides // Journal of Materials Science. – 2015.

23. Ohsumi S., Sato Y.J., Okazaki R. Transverse thermoelectric conversion in the mixed-dimensional semimetal WSi_2 // PRX Energy. – 2024. – Vol. 3. – Art. 043007. https://doi.org/10.1103/PRXEnergy.3.043007

24. Tao X., Jund P., Colinet C., Tedenac J. First-principles study of the structural, electronic and elastic properties of W_5Si_3 // Intermetallics. – 2010. – Vol. 18. – Pp. 688–693. https://doi.org/10.1016/j.intermet.2009.11.008

25. Isaev M.Sh., Khudayberdieva A.I., Mamatkulov M.N., Asatov U.T., Kodirov S.R. The surface layer morphology of Si⟨Cr⟩ samples // East European Journal of Physics. – 2024. – No. 4. – Pp. 297–300. https://doi.org/10.26565/2312-4334-2024-4-32

26. Benndorf C., Eckert H., Kösters J., Pöttgen R. Equiatomic transition metal (T) silicides TT′Si: systematics of ^{29}Si NMR Knight shifts // Zeitschrift für Naturforschung B. – 2024. – Vol. 79(12). – Pp. 583–594. https://doi.org/10.1515/znb-2024-0015

27. Benndorf C., Eckert H., Pöttgen R. ^{29}Si, ^{47}Ti, ^{49}Ti and ^{195}Pt solid-state MAS NMR spectroscopic investigations of ternary silicides TPtSi, germanides TPtGe (T = Ti, Zr, Hf) and stannide TiPtSn // Dalton Transactions. – 2016. – Vol. 45(19). – Pp. 8215–8223. https://doi.org/10.1039/C6DT00861E

28. Ponomarev I., Kroll P. ^{29}Si NMR chemical shifts in crystalline and amorphous silicon nitrides // Materials. – 2018. – Vol. 11. – Art. 1646. https://doi.org/10.3390/ma11091646

29. Stebbins J.F., Kelsey K.E. Anomalous resonances in ^{29}Si and ^{27}Al NMR spectra of pyrope ($[Mg,Fe]_3Al_2Si_3O_{12}$) garnets: effects of paramagnetic cations // Physical Chemistry Chemical Physics. – 2009. – Vol. 11. – Pp. 6906–6917. https://doi.org/10.1039/B904731J

30. Luković J. et al. Tungsten disilicide (WSi_2): synthesis, characterization and properties // Zeitschrift für Anorganische und Allgemeine Chemie. – 2017. – Vol. 643. – Pp. 329–337. https://doi.org/10.1002/zaac.201700329

31. Stoetzel J. et al. Microstructure and thermoelectric properties of Si–WSi_2 nanocomposites // Journal of Applied Physics. – 2017. – Vol. 121. – Art. 095101. https://doi.org/10.1063/1.4976836

32. Zhang S., Buchta R., Östling M. A study of silicide formation from LPCVD-tungsten films: film texture and growth kinetics // Journal of Materials Research. – 2001. – Vol. 16. – P. 88–96. https://doi.org/10.1557/JMR.2001.88

Information about authors:

Abdugafur T. Mamadalimov – Doctor of Physical and Mathematical Sciences, Academician, Head of the "Radiation Physics of Solids" Laboratory at the Institute of Semiconductor Physics and Microelectronics, National University of Uzbekistan named after Mirzo Ulugbek (Tashkent, Uzbekistan, e-mail: mamadalimov.edu@mail.ruMakhmudhodzha).

Makhmud Sh. Isaev – Doctor of Physical and Mathematical Sciences, Professor at the Department of Physics of National University of Uzbekistan named after Mirzo Ulugbek (Tashkent, Uzbekistan, e-mail: isayevmahmud02@gmail.com).

Sardor R. Kodirov – Lecturer at the Department of Interfaculty General Technical Sciences, Urgench State University (Urgench, Uzbekistan, e-mail: qodirov.sardor@urdu.uz).

Nilufar K. Khakimova – PhD, Senior Researcher at "Radiation Physics of Solids" Laboratory of the Institute of Semiconductor Physics and Microelectronics, National University of Uzbekistan named after Mirzo Ulugbek (Tashkent, Uzbekistan, e-mail: Khakimova_nilufar@mail.ru).

Ismoil A. Mengliev – PhD, Associate Professor at the Department of Applied Mechanics, Tashkent State University of Transport (Tashkent, Uzbekistan, e-mail: ismoilmengliyev399313@gmail.com).